The boundary of the N=90 shape phase transition: ^{148}Ce

IOP Conf. Series: Journal of Physics: Conf. Series **1023** (2018) 012022 doi:10.1088/1742-6596/1023/1/012022

The boundary of the N=90 shape phase transition: ^{148}Ce

P. Koseoglou [1,2], V. Werner [1,3], N. Pietralla [1], S.Ilieva [1], M. Thürauf [1], C. Bernards [3], A. Blanc [4], A. M. Bruce [5], R. B. Cakirli [6,7], N. Cooper [3], L. M. Fraile [8], G. de France [9], M. Jentschel [4], J. Jolie [10], U. Koester [4], W. Korten [11], T. Kröll [1], S. Lalkovski [12], H. Mach [13,†] , N. Mărginean [14], P. Mutti [4], Z. Patel [15], V. Paziy [9], Z. Podolyák [15], P. H. Regan [15,16], J.-M. Régis [10], O. J. Roberts [5], N. Saed-Samii [10], G. S. Simpson [17], T. Soldner [4], C. A. Ur [18], W. Urban [4], D. Wilmsen [9], E. Wilson [14]

[1] IKP TU-Darmstadt, Germany / [2] GSI, Germany / [3] Yale University, USA
[4] ILL Grenoble, France / [5] University of Brighton, UK / [6] MPIK Heidelberg, Germany
[7] Department of Physics, University of Istanbul, Turkey
[8] Universidad Complutense, Spain / [9] GANIL Caen, France
[10] IKP University of Cologne, Germany
[11] CEA, IRFU, Université Paris-Saclay, France
[12] University of Sofia "St. Kliment Ohridski", Bulgaria
[13] National Centre for Nuclear Research, Poland / [14] Horia Hulubei NIPNE, Romania
[15] University of Surrey, UK / [16] National Physical Laboratory, UK
[17] LPSC Grenoble, France / [18] INFN Legnaro, Italy

pkoseoglou@ikp.tu-darmstadt.de

Abstract. The even-even N=90 isotones with Z=60-66 are known to undergo a first order phase transition. Such a phase transition in atomic nuclei is characterized by a sudden change of the shape of the nucleus due to changes in the location of the potential minimum. In these proceedings we report a measurement of the $B_{4/2}$ ratio of ^{148}Ce, which will probe the location of the low-Z boundary of the N=90 phase transitional region. The measured $B_{4/2}$ value is compared to the prediction from the X(5) symmetry within the interacting boson model at the critical point between the geometrical limits of vibrators and rigid/axial rotors. The EXILL&FATIMA campaign took place at the high-flux reactor of the Institut Laue Langevin, Grenoble, were ^{235}U and ^{241}Pu fission fragments were measured by a hybrid spectrometer consisting of high-resolution HPGe and fast $LaBr_3$(Ce)-scintillator detectors. The fast $LaBr_3$(Ce) detectors in combination with the generalized centroid difference method allowed

lifetime measurements in the picosecond region. Furthermore, this kind of analysis can serve as preparation for the FATIMA experiments at FAIR.

1. Introduction-Motivation

The even-even N=90 isotones with Z=60-66, present an interesting phenomenon, known as shape-phase transition. This phase transition in atomic nuclei is characterized by a sudden change of the shape of the nucleus due to changes in the location of the potential minimum [1]. Both the characteristic level schemes and transition strengths, or their ratios, are fingerprints of the location of an isotope within a phase transition region. As such, the $R_{4/2}=E(4^+_1)/E(2^+_1)$ and $B_{4/2}=B(E2; 4^+_1\rightarrow 2^+_1)/B(E2; 2^+_1\rightarrow 0^+_1)$ values are sensitive benchmarks for this type of structure of a given nucleus.

In F. Iachello's Physical Review Letter [4] a schematic representation of the lowest portion of the spectrum of X(5) symmetry is provided, which can be compared to experimental data. For ^{152}Sm and ^{150}Nd this is presented in R.F. Casten's Physical Review Letter [1] and reveals the X(5) flavor of the nuclei. This X(5) symmetry describes nuclei that are located on the critical point between spherical, U(5) and axially deformed shapes, SU(3). Using the adopted experimental data, the discussed phase transition can be observed in a $R_{4/2}$ plot of these isotopes over the neutron number (figure 1). The sharp transition in the gadolinium and samarium isotopic chains [1, 2, 3] from spherical nuclei ($R_{4/2}$=2-2.4) to deformed ones ($R_{4/2}$=3-3.33) around N=90 is less pronounced in the neodymium and cerium chains. The latter chains undergo a transitional $R_{4/2}$ ratio from spherical to deformed nuclei ($R_{4/2}$=2.93 and 2.86 for neodymium and cerium respectively) at N=90 and the transition from N=88 to N=90 is smooth. The $B_{4/2}$ ratio can give additional information on the shape of the nucleus ($B_{4/2}$=2 for spherical symmetry, $B_{4/2}$=1.4 for γ-rigid and γ-soft deformed). Figure 2 presents the $B_{4/2}$ ratio for gadolinium, samarium and neodymium isotopes as a function of the neutron number. The adopted data were used. While the transition from N=88 to N=90 from near spherical symmetry to quadrupole deformed shapes is sharp for gadolinium and samarium it is less so for neodymium.

As indicated in figure 3, the N=90 isotones lie near the X(5) prediction [4]. In the case of ^{148}Ce, located at the low-Z boundary of this phase transition, the $R_{4/2}$ ratio (2.86) matches the X(5) prediction of 2.91 [4]. The P-factor, introduced in [5], defined in terms of number of valence protons and neutrons (N_p,N_n) by: $P=(N_p\cdot N_n)/(N_p+N_n)$, reflects the strength of the valance p-n interaction (numerator) and the strength of the pairing interaction (denominator). As noted in [2], a typical p-n interaction in heavy nuclei is ~ 200 keV and the pairing interaction is of the order of 1 MeV. Empirically it is observed that the p-n interaction begins to dominate for P ~ 4 - 5, which provides a pathfinder to possible X(5) candidates. For ^{148}Ce, with 8 valence protons and 8 valence neutrons, P=4, making this isotope a candidate for an X(5)-like structure. One signature for such an X(5) symmetry, as mentioned above, would be the $B_{4/2}$ ratio, for ^{148}Ce that has not been measured to date.

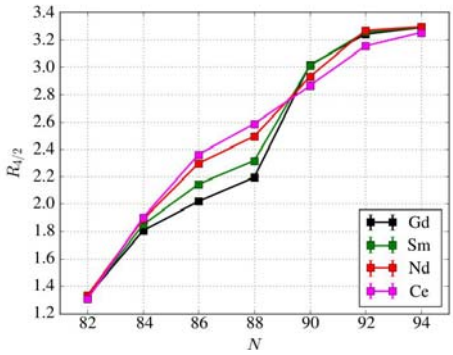

Figure 1. $R_{4/2}$ ratio over neutron number. The sharp transition of Gd and Sm from spherical nuclei ($R_{4/2}$=2) to deformed ones ($R_{4/2}$=3.33) is not present in Nd and Ce chains. Data taken from [6].

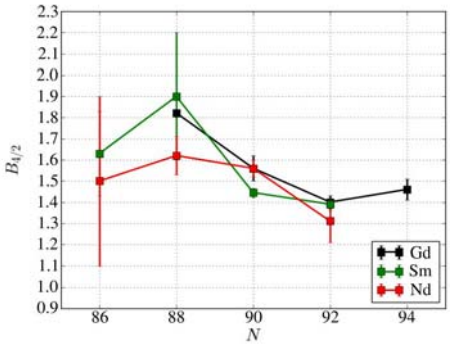

Figure 2. $B_{4/2}$ ratios for Gd, Sm and Nd isotopes as a function of neutron number. The transition from N=88 to N=90 from near spherical symmetry to γ-rigid and γ-soft symmetry is sharp for Gd and Sm but not for Nd. Data taken from [6].

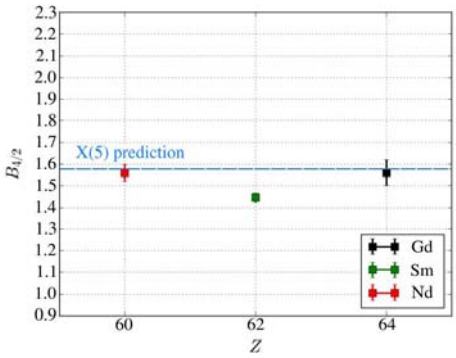

Figure 3. The $B_{4/2}$ ratio for N=90 isotones. All isotopes lie near the X(5) prediction. Data taken from [6].

2. Experiment

The EXILL&FATIMA campaign provided data for neutron-rich species in the vicinity of N=90. Using cold-neutrons fission of ^{235}U and ^{241}Pu was induced at the Institut Laue-Langevin (ILL) of Grenoble, France, and the prompt γ-rays coming from the nuclei in interest were detected using a hybrid array of HPGe and Ce-doped $LaBr_3$ detectors, the EXILL&FATIMA spectrometer. The EXILL array was composed of 8 BGO-shielded EXOGAM Clover detectors, each one consisting of 4 HPGe crystals, with a target-to-detector distance of 14.5 cm, placed at 90° relative to the beam direction, in ring arrangement. FATIMA consisted of 16 (5% Ce-doped) $LaBr_3$ detectors in two rings, at 40° and 140° relative to the beam direction. The efficiency of the $LaBr_3$ detectors was crucial for the experiment, so they were placed as close as possible to the target, resulting in a target-to-detector distance of 8.5 cm, almost touching each other. The neutron flux at the target position was approximately $9 \cdot 10^7$ n/cm^2·s. More details about the experimental setup can be found in [7].

All the fission fragments were stopped by the thick backing of the targets within ~1ps. More than 100 different isotopes were produced from the fission, thus multiple coincidences were utilized to separate an isotope of interest. Ge-$LaBr_3$-$LaBr_3$ coincidences were used to gate on the cascade of interest. The HPGe high-resolution detectors of the EXILL array allowed a precise energy gate to be set on a γ-ray cascade of interest and, hence, the nuclei of interest. The excellent timing performance of the $LaBr_3$ detectors in combination with the generalized centroid difference method allowed to measure lifetimes down to the ps range [8].

In this work the investigation at ^{148}Ce is presented.

3. Fast-timing measurements

As mentioned in the previous section the hybrid nature of the detector array allows both clean energy gates (using the HPGe detectors of EXILL) and fast-timing measurements (using the the fast $LaBr_3$ detectors of FATIMA). The Ge selection gates were placed in the same cascade as the level of interest but not on its feeder or decay gammas. The FATIMA detectors were used to measure the lifetimes of these levels. The $LaBr_3$ detectors were connected to the TACs in such a way that it allowed to know which of the two prompt gammas (decay or feeder) was the one providing the start or stop signal. In total 15 TACs were used (N-1, with N the number of $LaBr_3$ detectors) in such a way that TAC_i was able to be started by detector *i* and to be stopped by detector *j*, with *j*>*i*. A detailed description of the electronics setup used in the experiment can be found in Ref. [7].

Two time-difference spectra can be produced depending on whether the decay gamma ray is providing the start (start spectrum) or stop (stop spectrum) signal (whether the feeder gamma ray is providing the stop or start signal respectively). In the start spectrum the centroid (C_{start}) is shifted, by one lifetime, on the left direction, in the stop spectrum the centroid (C_{stop}) is shifted on the right direction. In figure 4 (adapted from [8]), a simpler case of this experimental setup together with the two corresponding time-distribution spectra are presented. The time spectra presented corresponds to a short lifetime in the ps range, this is the reason for the two prompt-shaped time distributions. The lifetime derives from the centroid difference (ΔC), see section 3.2. In a case of a long-lived state, a slope appears on one side of the spectrum, see section 3.1, and the slope corresponds to the lifetime.

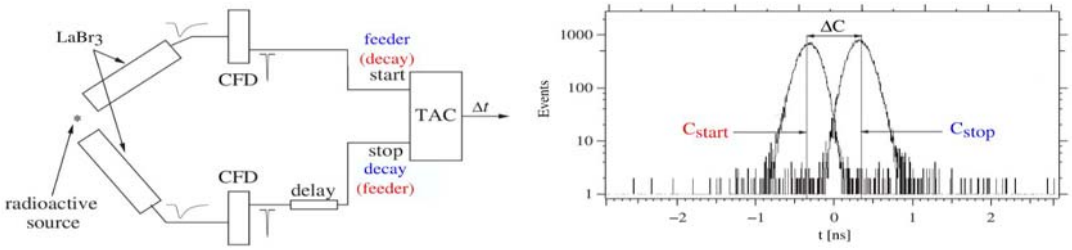

Figure 4. A simpler case of this experimental setup of just two detectors and the two time-distribution spectra are presented. Two time spectra can be produced depending on whether the decay gamma is providing the start (with the corresponding centroid, C_{start}) or stop (with the corresponding centroid, C_{stop}) signal (whether the feeder-gamma is providing the stop or start signal respectively).

3.1 2^+_1 lifetime using the slope method

For the 2^+_1 state, the slope method [9,10] was used due to the long lifetime in the order of ns. A Ge energy gate, on the decay gamma ray of the $6^+_1 \rightarrow 4^+_1$ transition, has been used for the selection of the cascade of interest. The start and the stop signals to the TACs were given by the feeder and the decay gamma of the 2^+_1 state and detected with FATIMA. After the Ge gate was performed, the feeder gamma ray ($4^+_1 \rightarrow 2^+_1$ transition) was set as the stop signal and the decay gamma ray ($2^+_1 \rightarrow 0^+_1$ transition) as start signal. Two background cuts on the right and left of the feeder gamma ray performed for Compton and random background subtraction from the time-difference spectrum. In figure 5 the resulting time-difference spectrum is shown. A clear slope was observed, corresponding to the lifetime of the state. The lifetime measured [11] was in agreement with the literature value [12], giving confidence in our method of handling the Compton and random background.

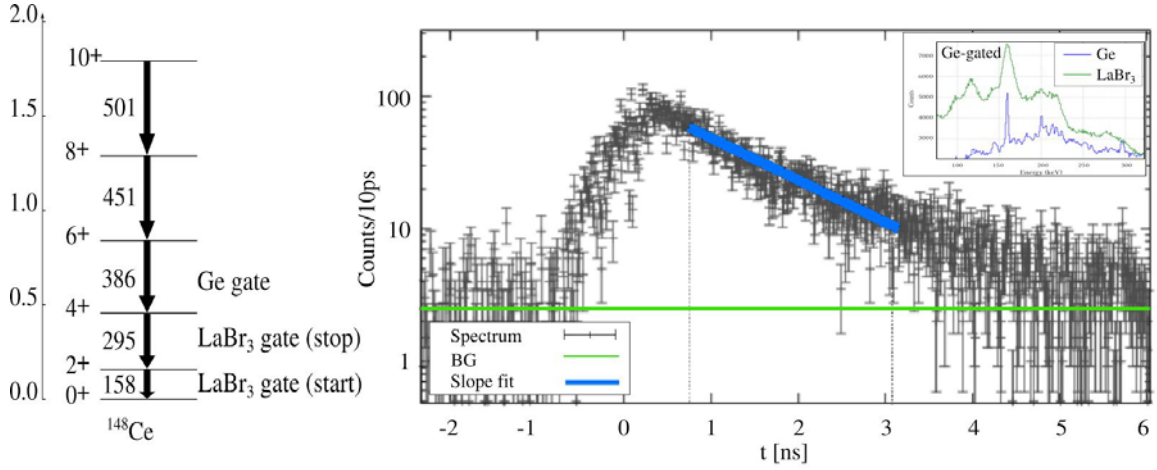

Figure 5. Start time spectrum, after performing the two background cuts. A clear slope can be seen. The slope corresponded to the lifetime of the state. The lifetime measured tagreed with the literature value [12]. The Ge-gated $LaBr_3$ (green) and Ge (blue) spectra can be seen on the top right. On the left side the level scheme is presented and the gates performed are indicated.

3.2 4^+_1 lifetime using the Generalized Centroid Difference method

For the 4^+_1 state the generalized centroid shift method [13] has been used for the determination of the lifetime (in the ps range). A Ge energy gate was set on the decay gamma of the 2^+_1 state to select the cascade of interest. The start and the stop spectra were produced by gating the decay gamma ray on the start and stop signal respectively (gatting the feeder gamma ray on the stop and start signal respectively). From the centroid difference (ΔC), of the centroids of the two time-difference spectra produced (see figure 7), the lifetime (τ) of the state could be measured. From using

$$\tau = (\Delta C - PRD) / 2 \ ,$$

where the prompt response difference ($PRD=PRD(E_{feeder}-E_{decay})=PRF(E_{feeder})-PRF(E_{decay})$) is reflecting the different time that the setup requires to record gammas with different energies (the so-called time walk). The prompt response function (PRF) was calibrated by measuring known cascades from a ^{152}Eu source and the $^{48}Ti(n,\gamma)^{49}Ti$ reaction. In figure 6 the produced PRF can been seen, adjusted for the reference energy of 342 keV. A precise description of the PRD calibration procedure is given in [14]. The Compton contribution to the time spectrum has been eliminated by performing two background cuts on the right and the left of the feeding gamma peak and subtract the mean time spectrum from the

time spectrum produced by cutting on the peak. The two time-spectra (start and stop) are shown in figure 7, together with the centroids.

From the measured lifetimes the B(E2; $4^+_1 \rightarrow 2^+_1$) and B(E2; $2^+_1 \rightarrow 0^+_1$) were calculated to be 140 (7) W.u. and 88 (3) W.u. [11] respectively, the $B_{4/2}$ ratio was calculated to be 1.6 (1), very near to the X(5) prediction (figure 8). In Ref. [15], an early state of the analysis was presented; quadruple coincidences have been used (Ge-Ge-$LaBr_3$-$LaBr_3$) for the measurement of the 4^+_1 lifetime. Beside the low statistics on the quadruple-gated case, which resulted in a large uncertainty, the $B_{4/2}$ ratios detected through the two methods (triple and quadruple gates) are in agreement, within the errors.

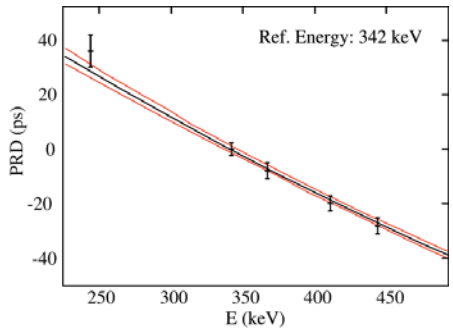

Figure 6. The prompt response function (PRF), adjusted for the reference energy of 342 keV, has been calibrated by measuring known cascades from a ^{152}Eu source and the ^{48}Ti(n, γ)^{49}Ti reaction.

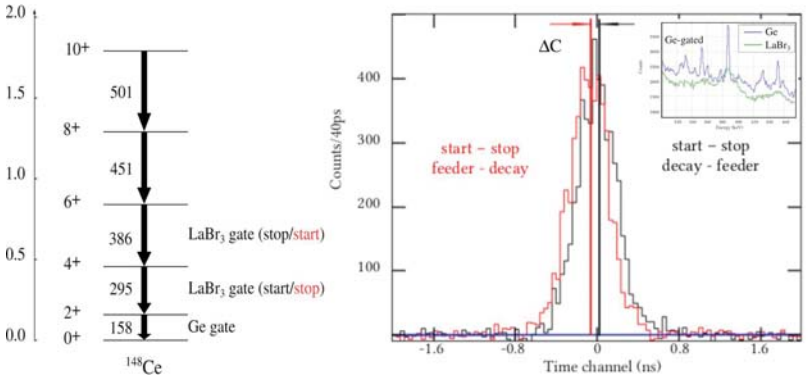

Figure 7. The two time-spectrum (start and stop), the centroids are also pictured. By measuring the lifetime the $B_{4/2}$ ratio was calculated. Also the Ge-gated $LaBr_3$ (green) and Ge (blue) spectra can be seen on the top right. On the left side the level scheme and and the gates selected are indicated.

4. $B_{4/2}$ ratio – X(5) character of ^{148}Ce

By measuring the 4^+_1 lifetime for first time, the the $B_{4/2}$ ratio was obtained, after correction for internal conversion. The calculated $B_{4/2}$ ratio is very near to the X(5) symmetry prediction for nuclei on the transition phase between spherical, U(5) and axially deformed shapes, SU(3). Plotting the energy levels emanating from X(5) and the experimentally measured in ^{148}Ce side by side (figure 8, left), one can perceive the good agreement between them.

^{148}Ce seems to follow the N=90 isotones' picture of the X(5) symmetry. In figure 8 one can witness the trend over the isotones. Together, all the above can designate ^{148}Ce as a good X(5) candidate.

Further indicators for the X(5) symmetry would be additional transition strengths' ratios, that were not obtained from the experimental data due to low statistics on higher excited levels.

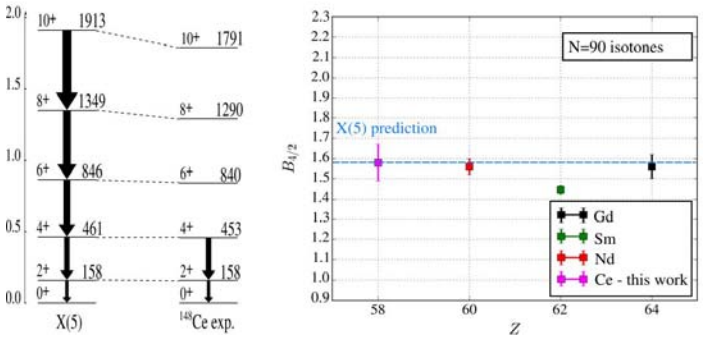

Figure 8. $B_{4/2}$ ratio of N=90 isotones. ^{148}Ce seems to follow the X(5) trend of the rest isotopes. Data, except for ^{148}Ce, taken from [8]. On the left the comparison between the X(5) prediction for the energy levels (normalized to the 2^+_1 state) and the experimental values is presented.

Acknowledgments

The EXILL&FATIMA campaign would not have been possible without the support of several services at the ILL and the LPSC. We are grateful to the EXOGAM collaboration for the loan of the detectors,to GANIL for assistance during installation and dismantling, and to the FATIMA collaboration for the provision of LaBr3 (Ce) detectors and analogue electronics.

This work was supported by the cooperation between TU Darmstadt and the GSI Helmholtz Center for Heavy Ion Research and by HGS-HIRe, by US DOE under No. DE-FG02-91ER-40609, by STFC (UK) under No. ST/L005743/1 and ST/G000751/1, by Istanbul University Scientific Research Project No. 54135, by DFG under No. KR 1796/2-1 and KR 1796/2-2 and by BMBF under No. 05P12RDNUP 05P15RDFN1, 05P15PKFNA and 05P12PKNU.

References

[1] R. F. Casten and N. V. Zamfir, Phys. Rev. Lett. **87**, 052503 (2001).
[2] R. F. Casten, Nature Physics **2**, 811 (2006).
[3] N. Pietralla and O.M.Gorbachenko, Phys. Rev. C **70**, 011304 (2004).
[4] F. Iachello, Phys. Rev. Lett. **87**, 052052 (2001).
[5] R. F. Casten, D. S. Brenner and P. E. Haustein, Phys. Rev. Lett. **58** 658 (1987).
[6] Nuclear Data Sheets, http://www.nndc.bnl.gov/ensdf/
[7] J.-M. Régis, et al., Nucl. Instr. and Meth., A **763** 210 (2014).
[8] J.-M. Regis, et al., Nucl. Instr. and Meth., A **622** 83 (2010).
[9] P. C. Simms, N. Benczer-Koller and C. S. Wu, Phys.Rev. **121**, 1169 (1961).
[10] V. Werner, et al., Phys. Rev. C **93**, 034323 (2016).
[11] P. Koseoglou, et al., in preparation.
[12] N. Nica, Nuclear Data Sheets **117**, 1 (2014).
[13] J.-M. Regis, et al., Nucl. Instr. and Meth. A **726** 191 (2013).
[14] J.-M. Regis, et al., Nucl. Instr. and Meth., A **684** 36 (2012).
[15] P. Koseoglou, et al., Lifetime of the 4^+_1 state of ^{148}Ce and its $B_{4/2}$ ratio. In: 3rd one-day workshop on New Aspects and Perspectives in Nuclear Physics. [online] Athens: Hellenic Institute of Nuclear Physics, pp.43 (2016).